IEEE Open Journal of Intelligent Transportation Systems

Received 18 February 2020; revised 7 April 2020; accepted 28 April 2020. Date of publication 30 April 2020; date of current version 19 May 2020.

Digital Object Identifier 10.1109/OJITS.2020.2991402

Optoelectronic and Environmental Factors Affecting the Accuracy of Crowd-Sourced Vehicle-Mounted License Plate Recognition

M. C. RADEMEYER, A. BARNARD, AND M. J. BOOYSEN

Department of Electrical and Electronic Engineering, Stellenbosch University, Stellenbosch 7600, South Africa

CORRESPONDING AUTHOR: M. J. BOOYSEN (e-mail: mjbooysen@sun.ac.za)

This work was supported by Southern African Transportation Conference.

ABSTRACT License plate recognition (LPR) technology has been used to combat vehicle-related crime in urban areas in many developed contexts. However, commercially available LPR systems are expensive and not feasible for large scale adoption in developing countries. The development of a low-cost crowd-sourced solution requires an informed approach to the selection of an appropriate camera, as well as a realistic understanding of the system's performance under various environmental conditions. This work investigates the effect of optoelectronic and environmental factors on the ability of a vehicle-mounted LPR system to correctly identify license plates, specifically for a mass-deployment crowd-sourced scenario. A theoretical LPR camera model was developed to estimate the effect of different cameras, while the effects of motion, orientation and lighting were evaluated in a series of experimental tests. The most influential optoelectronic factors were shown to be focus, focal length and image sensor resolution. Furthermore, recognition was impaired during high-speed turn maneuvers, angling of license plates away from the camera and certain night-time conditions. The optoelectronic model proved useful for the selection of a cost-effective camera for use in an open-source LPR system. Moreover, the study of environmental factors provided valuable insight into the limitations of LPR systems in various environmental and traffic conditions.

INDEX TERMS Crowdsourcing, number plate recognition, law enforcement, developing countries, operating conditions, optical specifications.

SYMBOLS USED

OPTOELECTRONIC

α_d	Diagonal angle of view
α_h	Horizontal angle of view
β	License plate horizontal apparent angle
C	Maximum allowable circle of confusion diameter
C_{factor}	Circle of confusion factor
d	Image sensor diagonal length
D_F	Depth of field far boundary
D_N	Depth of field near boundary
f	Lens focal length
H	Hyperfocal distance
N	Aperture f-number
R_{plate}	Horizontal license plate resolution
$R_{plateMin}$	Minimum horizontal license plate resolution
R_{sensor}	Horizontal image sensor resolution
S_{ext}	Lens extension
S_{focus}	In-focus distance
S_{sensor}	Lens to sensor distance
w	Image sensor width.

ENVIRONMENTAL

$\dot{\theta}$	Camera angular velocity in degrees
ϕ	Degrees of slant distortion
r	Camera turn radius
v	Camera velocity.

I. INTRODUCTION

EVERY 10 minutes a motor vehicle is stolen in Brazil while in South Africa an average of 44 vehicles are hijacked every day [1], [2]. In India, rash driving is the

most reported offense resulting in human harm [3]. These statistics provide a glimpse into the reality of vehicle-related lawlessness rampant in today's developing cities.

Many law enforcement agencies across the world have successfully employed license plate recognition (LPR) technology to crack down on vehicle-related crime – Approximately 71% of American law enforcement agencies use LPR technology [4] and Australian highway patrols daily catch multiple unregistered vehicles using LPR systems mounted on their patrol cars [5].

However, developing countries are prevented from harnessing the benefits of large scale LPR deployment due to commercially available systems generally being expensive, heavily reliant on proprietary technology and only offered as part of extensive comprehensive system solutions. In such countries, a scalable low-cost open-source LPR system would enable the crowdsourcing of traffic monitoring and vehicle tracking to civilian vehicles, which could leverage their mobility to double up as ubiquitous 'eyes on the road'. Centrally aggregating this information could greatly contribute to community safety and effective law enforcement in developing countries.

The development of such a system would require an informed selection of an appropriate camera for use with readily available hardware and software. Additionally, the expected performance of such a system in various conditions should be established.

License plate recognition technology is employed throughout the world to identity motor vehicles. An LPR system typically comprises a digital camera, which captures a scene containing the license plate, and a processing unit with a recognition algorithm, which is used to extract the license plate characters from the photograph [6]. LPR systems are commonly used in automatic speed enforcement, neighborhood security, vehicle theft management and many other related scenarios that require vehicle identification. Commercial LPR systems can offer accurate recognition up to a range of 30 m, although this varies greatly depending on the quality of the components [7]. Some systems are capable of recognizing license plates traveling at speeds up to 250 km/h [8]. These metrics help describe recognition accuracy, and as such are important considerations when selecting an appropriate LPR system.

The camera can be mounted in a static position to monitor vehicles driving past a specific location, such as a free-flow highway toll plaza or an access gate [9]. Such systems are generally permanent installations, having a dedicated lane or area to monitor and making use of sensors to detect the presence of vehicles. LPR systems are also commonly mounted on-board vehicles, typically on the dashboard, windshield or roof. This configuration allows license plates to be recognized while the vehicle drives through traffic and such mobility, if scaled, facilitates the monitoring of an extensive road network [10].

There is a large range of algorithms available for use in LPR solutions. Some high-end packages are proprietary and require a once-off payment or subscription fee in exchange for a highly optimized recognition algorithm [11], [12], while others are open-source and free [13], [14]. The typical algorithm consists of four basic stages: image acquisition, license plate detection, character separation and character identification [15].

The recognition process starts with the capture of the scene as a digital image. The image file is subsequently programmatically scrutinized to detect the presence and location of any license plates it may contain. This is commonly done using detection using the Canny, Sobel or Hough transform algorithms [15], [16].

Once a potential license plate has been identified, each character within it is isolated in preparation for individual recognition. Common techniques for this include the vertical projection and connected domain approach [17], [18]. The individual character images are then classified using a database of character images taken in various conditions and from different perspectives. Such a database will be specific for a regional license plate style. After each character is classified, the resulting license plate number is output as a single text string.

All these stages rely on the sharp contrast between the license plate's light-colored background and dark-colored characters and border. Image processing techniques may also be applied to pre-process and optimize images for recognition [19].

Various LPR systems exist in both infrastructure-based and vehicle-based manifestations. These tend to form part of large system solutions for centralized agencies in developed countries. However, to the best of the authors' knowledge, there exists no evaluation of the factors that impact the performance of vehicle-mounted LPR solutions, especially for its deployment in a crowd-sourced vehicle-tracking solution. We investigate how, and to what extent, (1) optoelectronic and (2) environmental factors affect the overall ability of vehicle-mounted LPR systems to correctly identify license plates. This ability is referred to as the system's recognition accuracy. Optoelectronic factors were evaluated due to the vast range of affordable compact cameras eligible for use in LPR systems, while the investigation into environmental factors was motivated by the highly dynamic and unpredictable nature of urban traffic conditions. Together, these provide insights into the selection of an appropriate camera system for use in low-cost crowd-sourced LPR networks. This work does not assess the detection performance of LPR technologies, but rather provides a framework for, and results of assessing the operational envelope of LPR. Accordingly, we propose the Geometric Recognition Envelope as a performance metric, which can be used to choose a camera and configuration that is fit for purpose. Introductory work to that presented in this paper can be found in [20].

II. FACTORS THAT INFLUENCE LPR

A. OPTOELECTRONIC FACTORS

A digital camera is considered an optoelectronic system because it manipulates and electronically captures light. This section briefly introduces the various physical components of a camera involved in capturing a digital image. Such components are referred to as 'primary camera properties' and greatly affect the resultant image. Attributes of the captured image are also explored and are referred to as 'derived camera properties'. This section is intended as an overview and introduction of terms, while the detailed analysis of the impact on each is presented in the results section.

1) PRIMARY CAMERA PROPERTIES

The environment observed by the camera is referred to as the scene. Light from objects within the scene enter through the camera lens and is projected onto the digital image sensor. The projected light is referred to as an image and is electronically captured to produce a digital photograph. This entire process is governed by the primary camera properties.

1) Focal length: The focal length, which is an inherent property of each camera lens, describes to what degree the lens bends incoming light from objects within the scene, as shown in Figure 1. It is measured as the distance (f) in millimeters at which a lens concentrates light from an object in the scene at infinity far away [21]. Light from objects in the scene that are closer to the lens will concentrate further away from the lens.

2) Lens to sensor distance: Objects are captured in sharp focus when their incoming light is concentrated precisely on the image sensor [22]. This is the case when objects at a specific distance from the lens, defined as the in-focus distance, S_{focus}. A desired in-focus distance is achieved by appropriately adjusting the distance between the lens and image sensor, S_{sensor}, as illustrated in Figure 1. Extending the lens further away from the sensor will bring closer objects within focus. The relationship between S_{sensor} and S_{focus} is defined by the thin lens equation as shown in Equation (1) [23].

$$\frac{1}{S_{focus}} + \frac{1}{S_{sensor}} = \frac{1}{f}. \tag{1}$$

3) Image sensor: Light projected onto the image sensor is subsequently electronically captured. The image sensor is covered by an array of photosensors, each producing an electronic charge proportional to the intensity of light falling on it. This charge is sampled and converted into a digital image using either complementary metal-oxide-semiconductor (CMOS) or charge-coupled device (CCD) technology. The total number of photosensors on an image sensor is referred to as the resolution. A resolution of 1920x1080 pixels is common in commercial LPR cameras [8], [24]. Large resolution generally corresponds to a large image sensor size. Sensor size is commonly expressed as a 'type' with a unit of optical format inches (e.g., a type 1/3.2″ sensor).

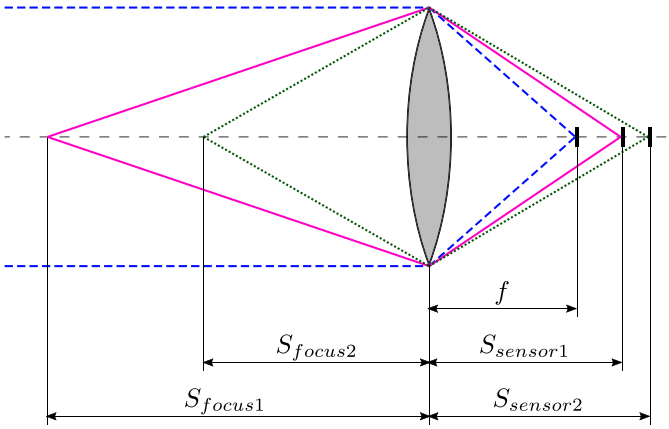

FIGURE 1. Illustration of a lens bending incoming light from objects at various distances. By adjusting S_{sensor}, light from an object at a specific distance (S_{focus}) will be concentrated on the image sensor, resulting in these objects being captured in-focus.

Compact cameras commonly employ a rolling shutter technique in which each row of photosensors starts to accumulate charge as soon as the previous row has been read out digitally. The delay between the start of each row's exposure is equal to the row readout delay and is determined by the ADC (analog to digital converter) speed. The sequential exposure of rows gives rise to undesirable slant distortion when capturing fast-moving objects.

The duration for which each row is set to accumulate charge is referred to as the intergeneration time. This is typically increased in low-light conditions to allow a sufficient amount of charge to be accumulated. However, any movement of incoming light during this period will result in light spreading over additional photosensors, a phenomenon known as motion blur.

4) Aperture: The camera aperture physically restricts the amount of light entering the camera [25]. The aperture size can be adjusted by varying the f-number setting. The diameter of the aperture opening will be equal to the focal length divided by the selected f-number. A large f-number will therefore imply a small aperture opening for a given focal length, allowing less light onto the image sensor.

2) DERIVED CAMERA PROPERTIES

The captured image will exhibit certain characteristics based on the primary camera properties involved in its capture. Such derived camera properties include angle of view, depth of field and object resolution.

1) Angle of view: The angle of view (AoV) is the solid angle describing the portion of the scene captured by the camera. A wide AoV captures a greater area of the scene and may produce barrel distortion, while a narrow-angle of view produces a zoomed-in image of a small area within the scene. The AoV measured diagonally across the scene (α_d) is dependent on the image sensor diagonal (d) and focal

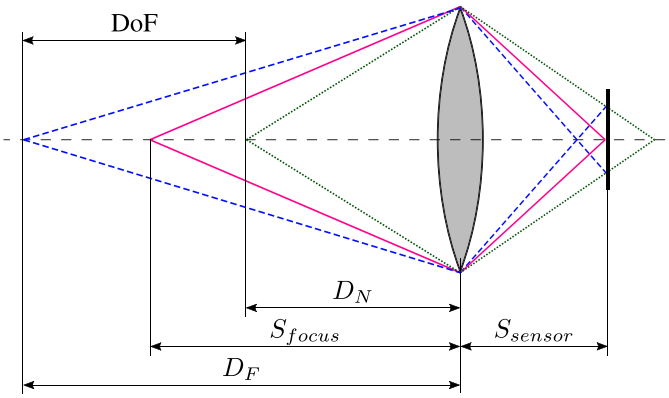

FIGURE 2. Illustration of the DoF. It is noteworthy that only light from objects positioned at S_{focus} (solid line) will be concentrated precisely on the image sensor.

length (f), as shown in Equation (2) [23].

$$\alpha_d = 2\arctan\left(\frac{d}{2f}\right). \tag{2}$$

2) Depth of field: The region in which objects can be captured sufficiently in focus is referred to as the depth of field (DoF) [22]. The size of the depth of field is determined by a near (DoFN, D_N) and far (DoFF, D_F) boundary, as illustrated in Figure 2. The distance to each boundary can be calculated based on the in-focus (S_{focus}) and hyperfocal (H) distances, as shown in Equation (3) and (4) [26].

$$D_N = \frac{HS_{focus}}{H + S_{focus}} \tag{3}$$

$$D_F = \frac{HS_{focus}}{H - S_{focus}} \tag{4}$$

The hyperfocal distance is equal to the in-focus distance producing the largest DoF. The DoFF will approach infinity for any in-focus distance greater than or equal to the hyperfocal distance. The hyperfocal distance can be calculated based on the focal length (f), aperture size in f-number (N) and maximum allowable circle of confusion diameter (C), as shown in Equation (5) [26].

$$H = f + \frac{f^2}{NC}. \tag{5}$$

3) Object resolution: Object resolution describes the number of pixels representing individual objects within the scene. Incoming light from the scene will cover an area of the image sensor proportional to the apparent size of each object within the scene. Depending on the sensor resolution, this area will cover a certain number of photosensors, each producing a pixel in the captured image. In the context of LPR, license plates consisting of minimum of 30 pixels in height can be accurately recognized, depending on the algorithm used [27].

B. ENVIRONMENTAL FACTORS

Recognition accuracy is also influenced by the environment in which LPR systems operate. Vehicle-mounted systems are subject to additional factors, which can generally be controlled in static applications. Three of the factors, namely relative motion, relative orientation and lighting, constantly change throughout the operation of a vehicle-mounted system, and are known to impact recognition accuracy [27]. The effect of environmental factors is preserved in the captured image and can generally be characterized by the resulting distortion. Each type of distortion poses a unique challenge to the recognition algorithm.

1) RELATIVE MOTION

In the hyperdynamic environment of vehicle-mounted LPR, both cameras and license plates constantly change position, speed and move across on the road. When a camera and license plate move at different velocities or trajectories the effect of relative motion is captured by the camera. Two common distortions resulting from relative motion are motion blur and slant.

1) Motion blur: Motion blur typically occurs when moving objects are captured in low-light conditions due to the longer integration time needed to capture a sufficient amount of incoming light. Motion blur is problematic for LPR due to the blur of the license plate and character edges. The lack of sharp, high-contrast edges severely limits the accuracy of the recognition algorithm.

2) Slant distortion: Another effect of relative motion, known as slant, occurs when a camera with a rolling shutter captures a license plate moving horizontally across the scene. Due to the photosensor row readout delay, each row will capture the license plate an instant after the previous row. A rapidly moving license plate will therefore appear to progressively shift in sequential rows. When stacked together in the final image, this shifting results in a slanted license plate. This effect is even greater in high-resolution sensors, where objects are captured by more rows. The slanting of license plate characters impair accurate character segmentation and recognition.

2) RELATIVE ORIENTATION

The relative orientation of the license plate and camera also influences the recognition accuracy. A license plate not precisely aligned towards the camera lens will result in a distorted license plate being captured. When sufficiently distorted, the algorithm will be unable to accurately recognize the license plate. The type of perspective distortion can be characterized based on the axis on which the license plate is rotated away from the camera. Commercial LPR systems can tolerate some perspective distortion, such as a yaw angle of 15° and a pitch angle of 30° [27].

3) LIGHTING CONDITIONS

Urban driving occurs in many different lighting conditions. Ambient light intensity varies greatly based on weather conditions and time of day, while artificial lighting may introduce directional light beams at specific wavelengths.

To aid in night-time visibility, most license plates feature a retroflective background. This reflects light directed at the license plate back towards the source, producing a high contrast between the reflective background and dark characters. An LPR camera mounted on a vehicle is ideally located to capture light retroflected from the vehicle headlights. Conversely, on-coming headlights may produce lens flare and glare which impair recognition. These are caused by internal reflections within the camera lens and may obscure license plates within the captured image.

III. MODEL

Using a mathematical optoelectronic model allowed us the opportunity to evaluate more camera properties than would practically feasible. We created the model by firstly identifying the photographic conditions necessary for successful number plate recognition. Each of these conditions was subsequently described in terms of a derived camera property and combined into a single metric. A theoretical framework was formulated to calculate the value of derived properties based on primary camera properties using fundamental optical formulas. Finally, the entire model was implemented as a software simulation.

A. RECOGNITION REQUIREMENTS

This analysis specifically considered a forward-facing dashboard-mounted LPR camera in a static and well-lit environment, thereby allowing the impact of optoelectronic factors to come to the forefront. The region in front of the camera in which license plates can be correctly identified was selected as a major aspect of recognition accuracy and defined as the recognition area. Certain photographic criteria have to be satisfied for a license plate to be recognizable. Three of these were considered in the mathematical model, namely that the license plate should be:

1) Wholly visible
2) Sufficiently focused
3) Captured with sufficient resolution

The first condition is self-explanatory, as a partially visible license plate would result in only some characters being recognized. Secondly, high contrast is required along character edges for accurate recognition to be possible. This necessitates that license plates be captured sufficiently in-focus. Lastly, license plates have to be captured with sufficient resolution for accurate character identification to be possible.

Each of these conditions corresponds to a respective derived camera property, namely AoV, DoF and object resolution. This allows the photographic criteria to be redefined in terms of these properties. A license plate could then be considered recognizable if it is:

1) Contained wholly within the AoV
2) Located within the DoF boundaries
3) Consisted of a predetermined minimum number of pixels

B. GEOMETRIC RECOGNITION ENVELOPE

The geometric recognition envelope (GRE) was defined as the boundary of the region in which license plates satisfied all three recognition requirements, and was used as the primary metric for the effect of optoelectronic factors on the recognition area. The shape of a GRE would be dependent on a camera's derived properties. Practically, it describes the estimated minimum and maximum recognition range and the extent to which license plates in adjacent lanes could be recognized. Using the GRE metric allows the model to be used as a tool for selecting an appropriate camera to achieve a desired recognition area (Shown in Figure 5).

C. THEORETICAL FRAMEWORK

A theoretical framework was formulated to calculate the derived camera properties based on primary properties describing the physical camera components. This would allow the GRE to be determined for any given camera.

1) ANGLE OF VIEW

The visibility requirement would be satisfied by license plates located completely within the horizontal AoV. This would determine the extent to which license plates in adjacent lanes were included within the GRE. The diagonal AoV equation (Equation (2)) was adjusted for horizontal AoV (α_h) by substituting image sensor width (w) for diagonal length, as shown in Equation (6). Hereafter, the term AoV will refer specifically to the horizontal AoV.

$$\alpha_h = 2\arctan\left(\frac{w}{2f}\right). \tag{6}$$

2) DEPTH OF FIELD

License plates would be captured in sufficient focus for accurate recognition if located within the DoF boundaries (Equations (3) and (4)). These are dependent on the in-focus (S_{focus}) and hyperfocal (H) distances, which are in turn determined by primary camera properties.

Equation (1) can be used to derive the in-focus distance from the distance between the lens and image sensor (S_{sensor}) and the focal length (f). The distance that the lens was extended past the focal length was defined as the lens extension (S_{ext}), as depicted in Figure 3 and Equation (7). Such a definition would allow lens extension to be analyzed independently of focal length, affording greater insight into the effect of the two individual properties. Substituting this definition into Equation (1) provided a solution for S_{focus} in terms of two primary camera properties, as shown in Equation (8).

$$S_{sensor} = f + S_{ext} \tag{7}$$

$$S_{focus} = \frac{f^2}{S_{ext}} + f \tag{8}$$

The hyperfocal distance is dependent on the focal length, f-number and maximum circle of confusion diameter, as per Equation (5). The maximum circle of confusion diameter is a chosen threshold and not an inherent camera property. It

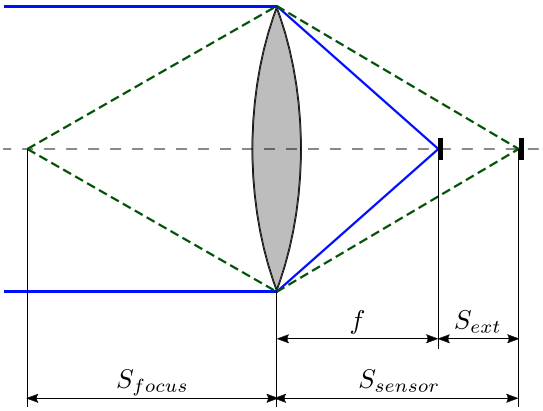

FIGURE 3. Illustration of S_{sensor} being extended past the focal length, resulting in a closer in-focus distance.

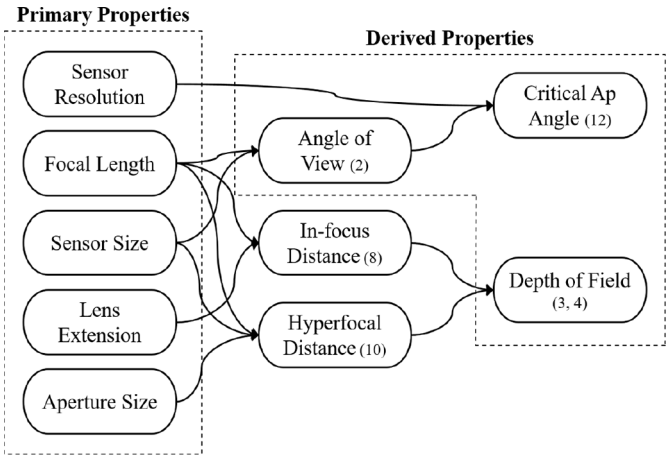

FIGURE 4. Mathematical dependency of derived camera properties on primary camera properties.

is commonly described as a fraction (C_{factor}) of the diagonal image sensor size, as shown in Equation (9). The GRE model used a C_{factor} of 1500, as is commonly used in the photographic industry [28]. This equation was substituted into Equation (5) to provide a solution for hyperfocal distance in terms of primary camera properties and the selected circle of confusion factor, shown in Equation (10).

$$C = \frac{d}{C_{factor}} \tag{9}$$

$$H = f + \frac{f^2 C_{factor}}{Nd}. \tag{10}$$

3) OBJECT RESOLUTION

License plates were required to occupy a minimum number of pixels for accurate recognition to be considered possible. This analysis relied on the perspective projection model used for modeling conventional non-fish-eye lenses common in LPR cameras [29]. The angle within the AoV occupied by the license plate was defined as the license plate's apparent angle (β). Light from the license plate would cover a certain number of horizontal sensor pixels (R_{plate}) out of the total horizontal sensor resolution (R_{sensor}). The fraction of the AoV occupied by the license plate would be equal to the fraction of horizontal sensor pixels occupied by the license plate, as per Equation (11).

$$\frac{\beta}{\alpha_h} = \frac{R_{plate}}{R_{sensor}} \tag{11}$$

By setting R_{plate} equal to the minimum number of horizontal pixels required for recognition ($R_{plateMin}$), β would describe the critical apparent angle (CAA) which a license plate should occupy for it to be captured with sufficient resolution, as shown in Equation (12). The theoretical model used an $R_{plateMin}$ of 140 pixels, based on the common recognition requirement of 30 vertical pixels and the aspect ratio of European Union (EU) license plates [27]. A license plate was considered to occupy sufficient resolution only if its apparent angle was wider than the CAA.

$$\frac{CAA}{\alpha_h} = \frac{R_{plateMin}}{R_{sensor}}. \tag{12}$$

D. IMPLEMENTATION

The theoretical model was implemented as a software simulation. Due to each derived property being dependent on multiple primary properties, it was necessary to consider the effect of all five primary properties in unison. By varying a single primary camera property, its effect on the derived properties and GRE could be observed. The mathematical dependency of the derived properties on primary camera properties is summarized in Figure 4. The numbers in parentheses indicate the equation by which each property could be calculated.

The GRE is the mutually inclusive region of the calculated AoV, DoF and CAA, as shown in Figure 5. The far range is limited by either the CAA or the DoFF, while the DoFN solely determines the near recognition range. Coverage of adjacent lanes is governed by the AoV. To appreciate the GRE of a vehicle-mounted camera, the GRE was plotted onto a virtual section of the road.

IV. EXPERIMENTAL SETUP

Real-world experiments were conducted to validate the theoretical optoelectronic model and determine the effect of environmental factors on LPR. A commercially available camera was selected based on primary property combinations readily available and producing the largest simulated GREs. The properties of the experimental camera are detailed in Table 1. The lens featured manual adjustment rings for variable focal length, aperture size and lens extension. This invaluable feature allowed the evaluation of different primary properties using a single camera, thereby maintaining a consistent test platform and minimizing cost.

The camera was connected to a Raspberry Pi single-board computer running generic image capture software, as well

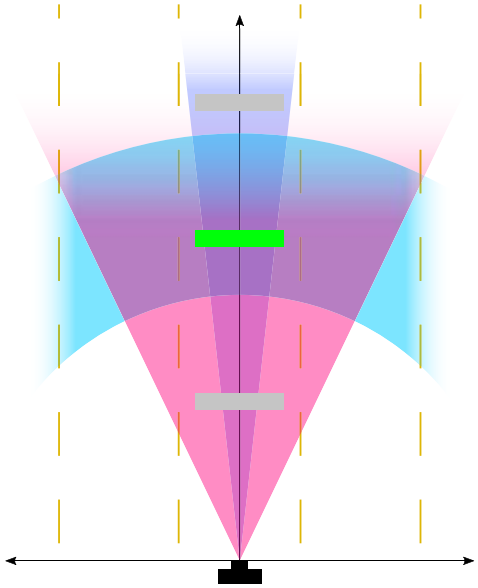

FIGURE 5. Illustration of how the AoV (red), DoF (cyan) and CAA (purple) determined the shape of the GRE and where license plates were classified as recognizable.

TABLE 1. Primary properties of the experimental camera.

Property	Value
Focal length	2.6 - 9 mm varifocal
Lens extension	Manually adjustable
Aperture	f/1.8 max opening
Sensor resolution	3264×2448 (8MP)
Sensor size	1/3.2" (5.7mm diagonal)

as OpenAlpr recognition software. Raspberry Pi's are inexpensive, readily available in developing countries and offer sufficient processing power for the execution of a recognition algorithm. Furthermore, Raspberry Pi's are also suited for use in vehicle-mounted applications, due to their compact size and sufficiently low-power rating. The Raspberry Pi was remotely controlled from a laptop via an Ethernet connection. The photographs and recognition results were stored locally on a microSD card.

The OpenALPR algorithm was used due to it being freely available,[1] widely supported and reliable. On average, the algorithm took 3.6 seconds to recognize a license plate in an 8MP image. The algorithm was implemented as a plug-and-play module and not modified in any way. The use of a stock algorithm served as a consistent recognition accuracy baseline for use in various testing conditions. Additionally, both algorithm classifier and license plate employed the EU format, thereby mitigating any recognition challenges related to a mismatch of license plate format. This enabled the analysis of factors independent of a recognition algorithm and license plate format.

The validation of the theoretical model entailed a license plate being captured at multiple static positions within an indoor venue with constant lighting using different camera

1. The OpenALPR source code can be download from https://github.com/openalpr/openalpr.

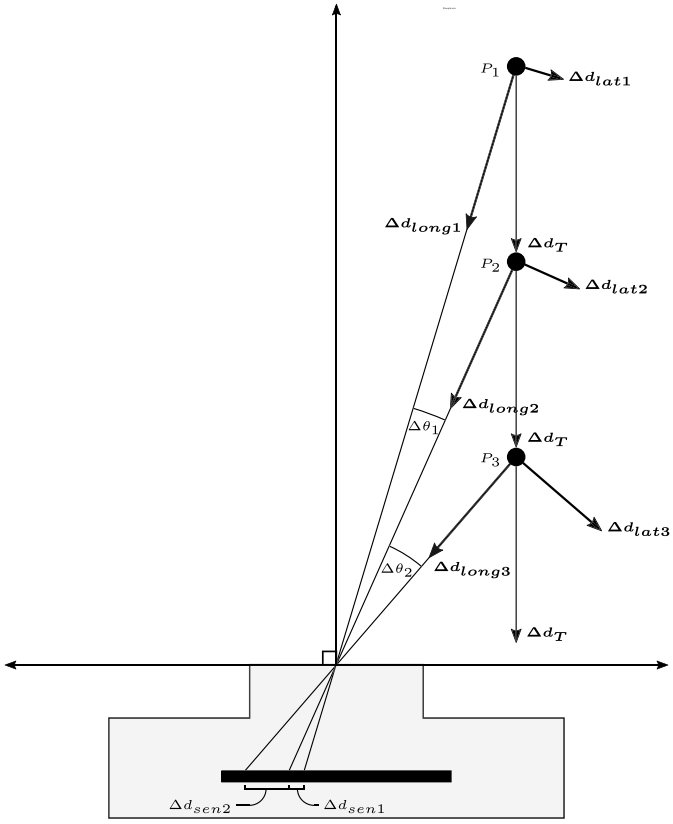

$P_{[n]}$	Object position
$\boldsymbol{\Delta d_T}$	Travel vector
$\boldsymbol{\Delta d_{long[n]}}$	Longitudinal motion component
$\boldsymbol{\Delta d_{lat[n]}}$	Lateral motion component
$\Delta\theta_{[n]}$	Angle rotated around camera
$\Delta d_{sen[n]}$	Distance moved on sensor

FIGURE 6. Relative lateral motion contributing to motion blur.

properties. The recognition area would be determined based on the positions at which the algorithm correctly identified the license plate. Multiple experiments were also designed to capture the distortion commonly caused by environmental factors, as further explained in this section.

A. RELATIVE MOTION

The effect of relative motion on recognition accuracy was analyzed by separating the motion into two orthogonal components: Motion towards or away from the camera was referred to as longitudinal motion, while motion that maintained the distance between the license plate and camera was termed lateral motion. This is illustrated in Figure 6 using the perspective projection model [17]. The figure illustrates an object traveling with constant velocity relative to the camera's principal axis, displayed at three positions with equal time and distance intervals. The travel vector consists of a longitudinal and lateral component. The lateral component relates to the angle rotated around the camera. This angle

corresponds to the distance moved by light from the object on the image sensor.

Given the equal time interval between positions, greater lateral motion would relate to a larger distance moved on the image sensor. This would relate to a greater amount of motion blur for a given integration time. From this, it was concluded that the lateral component of relative motion contributes to the phenomenon of motion blur. Furthermore, lateral motion is also responsible for producing slant distortion in rolling shutters cameras.

A lateral motion experiment requires strict control over the relative rotation of the license plate around the camera. This was achieved by placing the camera system on a single-axis rate table. A license plate, mounted on a static tripod, was positioned 5m away from the apparatus. Rotating the camera system clockwise at different angular velocities accomplished the relative license plate rotation required. The effect of lateral motion on recognition accuracy could be observed by capturing photographs at the instant the camera was aimed towards the license plate.

The effect of lighting on motion blur was incorporated by repeating the lateral motion experiment in two different lighting conditions: bright afternoon sunlight shining directly onto the face of the license plate and dim indoor florescent lighting similar to that produced by streetlamps.

B. RELATIVE ORIENTATION

The license plate can be rotated away from the camera on the pitch, roll and yaw axes. Significant pitch distortion may occur when a vehicle is positioned on a steep incline or a great height difference exists between the dashboard-mounted camera and a license plate. Roll distortion can impair recognition when vehicles are located on uneven terrain, such as one side of the vehicle parked over a curb. Such conditions occur less frequently than those producing yaw distortion. Common examples of yaw distortion include vehicles in adjacent lanes, those that parked perpendicular to the road or any vehicle turned away from the camera.

An experiment was designed to determine the effect of yaw rotation on recognition accuracy. The experiment was conducted in a large indoor venue, allowing constant ideal lighting conditions. Furthermore, the camera and license plate were mounted on static tripods to avoid the effect of relative motion being captured. The license plate was positioned in front of the camera and progressively rotated and captured at increments of 11.25° ($\frac{1}{32}$ of a full rotation).

C. LIGHTING CONDITIONS

Various light sources may illuminate license plates in urban traffic. The effect on recognition accuracy depends on the direction, intensity and spectrum of such light. Bright sunlight and moderate artificial light were already evaluated as part of the lateral motion experiment. Another commonly occurring condition is that of night-time driving. This condition features the use of directional light from vehicle headlights and allows the retroflective property of license plates to come to the forefront.

An experiment was designed to establish the effect of vehicle headlights and retroflective license plates on recognition accuracy. This involved setting up a pitch dark test environment in a large indoor venue. Two high-power incandescent lamps were positioned either side of the camera, reproducing the typical configuration of headlights and a dashboard-mounted camera. The measured recognition area was then compared to that achieved under ideal lighting conditions. Additionally, the effect of lens flare and glare were investigated by capturing images of real-world oncoming traffic at night.

V. RESULTS

A. OPTOELECTRONIC RESULTS

1) SIMULATION

A range of values were simulated for each primary property. The optoelectronic model clearly illustrated the effect of each primary camera property. This was complemented by results from the real-world test. In each case, the derived properties were calculated and GREs plotted. Only one property was varied at a time, allowing the effect of each property to come to the forefront.

1) Focal length: A change in focal length affected all three derived properties and thereby the overall shape of the GRE. Figure 7 shows the simulated GREs, along with derived properties, for a range of focal lengths. Increasing the camera focal length narrowed the AoV and CAA while extending the DoF further away from the camera, producing a long and narrow GRE with greater overall size when projected onto the road surface. This resulted in near license plates in adjacent lanes no longer being visible, but far license plate being captured in sufficient focus and resolution for accurate recognition.

The DoFF was identified as the limiting factor of the far range for a focal length of 5 and 7 mm, as evident from the maximum GRE range matching the DoFF. However, for greater focal lengths, the maximum range of the GRE was closer than the DoFF, implying that far range was instead determined by the CAA. This change was due to an increasing DoFF alongside a decreasing CAA. Both these trends allowed for greater far recognition range, due to further focus and a narrower allowable apparent angle, as illustrated in Figure 8. However, the DoFF changed at a greater rate than CAA, resulting in CAA becoming the limiting factor of the far range for focal lengths from 9 mm. At this point, the reason for limited far recognition changed from insufficient focus to insufficient license plate resolution.

2) Lens extension: Increasing the lens extension brought the in-focus distance closer and thereby shortened both DoF boundaries. This resulted in a small and near DoF, effectively shrinking the GRE size when projected onto the road surface, illustrated in the first two diagrams of Figure 9. Although this brought near license plates within focus, it also resulted in

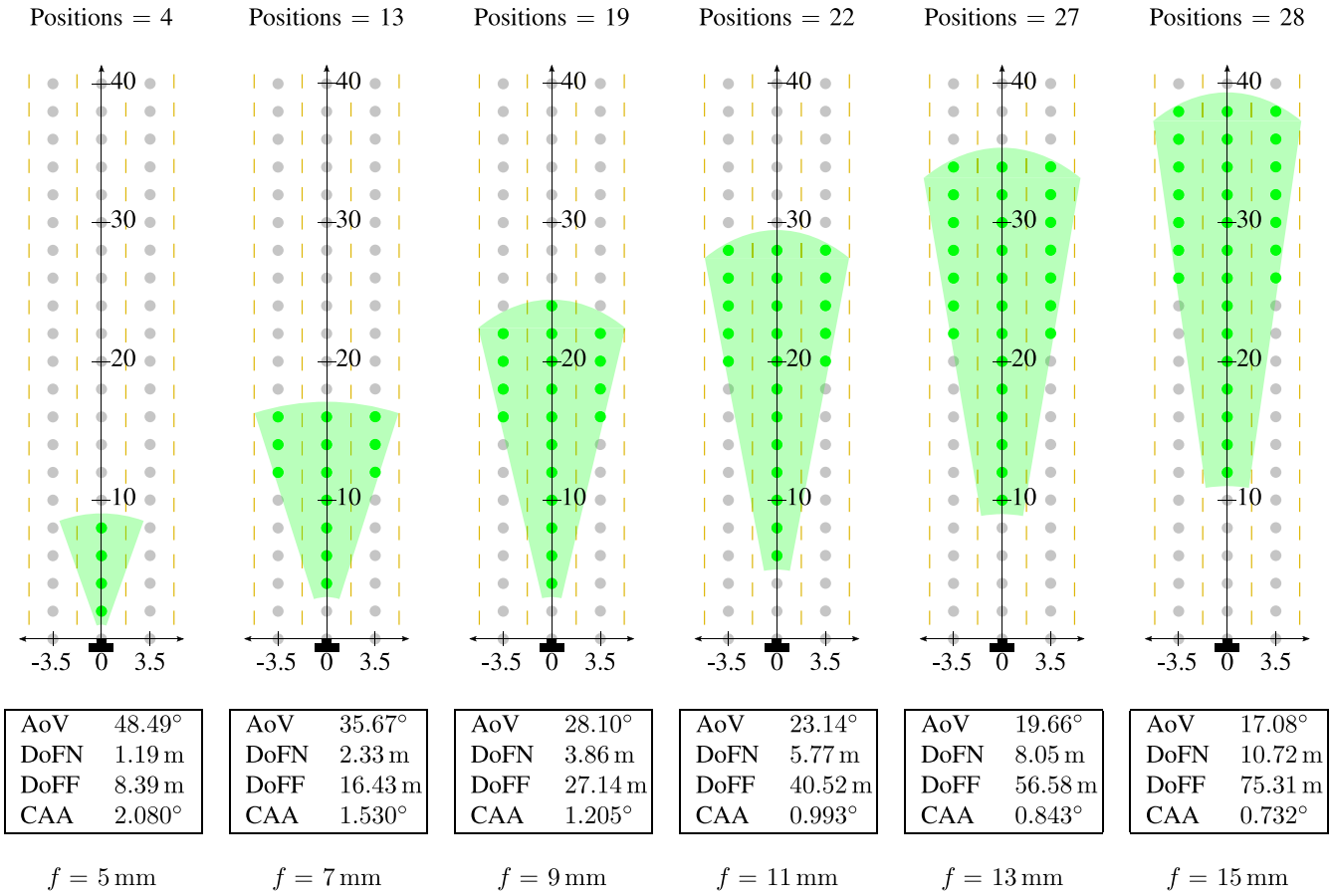

FIGURE 7. Simulated GREs and derived properties for various focal lengths (axis in meters).

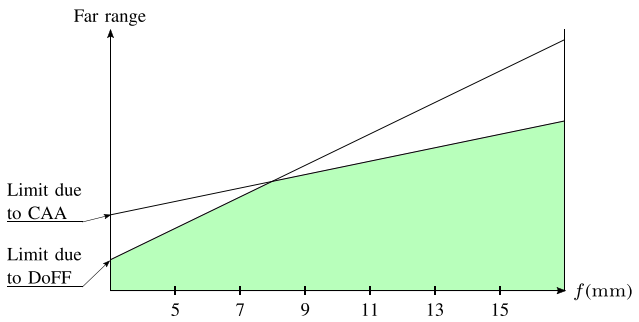

FIGURE 8. The relationship between CAA and DoFF as far range limiting factors for various focal lengths. The shaded region represents the GRE and is determined by the nearest limiting factor.

far license plates becoming out of focus. It is noteworthy that a large GRE could be achieved for a single lens extension. This indicates that the use of a fixed-focus lens may be sufficient for achieving a large recognition area. Such a lens will be a reliable and inexpensive alternative to an auto-focus lens.

3) Aperture size: The aperture size affected the hyperfocal distance and thereby the DoF boundaries. An increasing f-number, corresponding to a smaller aperture opening, extended the DoFF and shortened the DoFN. This resulted in a greater area being captured in sufficient focus for recognition, especially at far range, as shown in the middle two diagrams of Figure 9. It should be noted that a small aperture size may impair recognition accuracy in low light conditions.

4) Image sensor resolution: The use of higher resolution image sensors inversely proportionally decreased the CAA, thereby dramatically extending the far GRE's boundary. This allowed license plates to be capture with sufficient resolution at much greater range, as depicted in the final two diagrams of Figure 9.

5) Image sensor size: A variation of sensor size affected all three derived properties and gave rise to an interesting phenomenon. The simulated GREs are shown in Figure 10. An increasing sensor size slightly widened the AoV and CAA, shortened the DoFN and extended the DoFF. This produced a wider GRE with slight variance in far range.

It is noteworthy that the far recognition range fluctuated for increasing sensor size. This was due to both the DoFF and CAA increasing, creating an effect comparable to that observed in the focal length analysis and illustrated in Figure 11. In this case, an increasing DoFF extended the far range for sensor types 1/3.6″, 1/3.2″ and 1/3.0″, while the increasing CAA shortened the far range at larger sensor sizes. This relationship produced the rise and fall of far range seen in the simulated GREs.

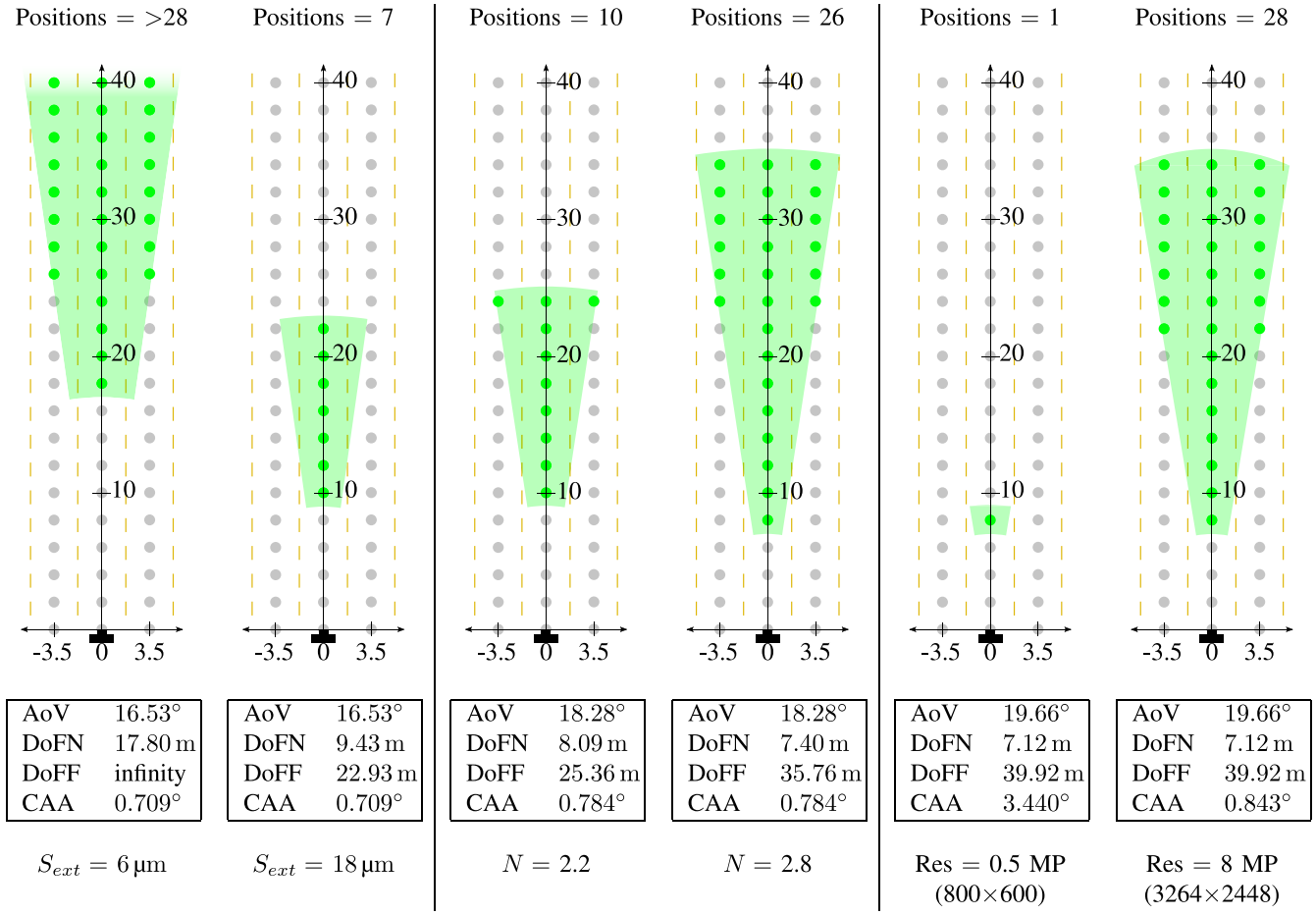

FIGURE 9. Simulated GREs for the maximum and minimum lens extension, aperture size and sensor resolution (axis in meters).

2) EXPERIMENTAL RESULTS AND MODEL VALIDATION

The experimental test provided a useful comparison between the theoretical model and real-world LPR cameras. Two camera configurations with different focal lengths were evaluated.

1) Short focal length: At short focal lengths the experimental camera system produced a recognition area almost identical to the simulated GRE. In both cases the far recognition range was limited by license plate resolution. The furthest experimentally recognizable license plate comprised only 135×28 pixels, a mere 3.6% less than the 140 horizontal pixels used as the theoretical recognition requirement.

However, near recognition range was limited by the DoFN in the simulation, but not in the experiment. Instead, photos of near license plates displayed signs of insufficient lighting and barrel distortion. Application of brightness and pincushion correction allowed these license plates to be recognized.

The insufficient lighting was attributed to the edge of the test range being poorly lit. On the other hand, barrel distortion occurs in cameras with large AoVs and affect the entire image. The amount of curvature is greater for objects far away from the center of the frame, with limited curvature occurring at the frame center. Because of this, the edges of a nearing license plate would at some point reach critical curvature at which recognition would fail.

2) Long focal length: The long focal length configuration also produced a recognition area similar to the simulated GRE, barring a slight difference in same-lane coverage. It is noteworthy that both regions featured identical coverage of adjacent lanes, validating the use of AoV in modeling the width of the recognition area.

Both the simulated and experimental far range was limited by license plate resolution. The furthest experimentally recognizable license plate consisted of only 120×25 pixels, 14% less than required in the theoretical model. This difference explained the longer range of the experimental recognition area.

The near recognition range was limited by the DoFN in the simulation. However, photographs of near license plates were well in-focus, but dark. By applying brightening correction, near license plates previously unrecognizable could be recognized. This established insufficient lighting as the near range limit of the experimentally measured recognition area.

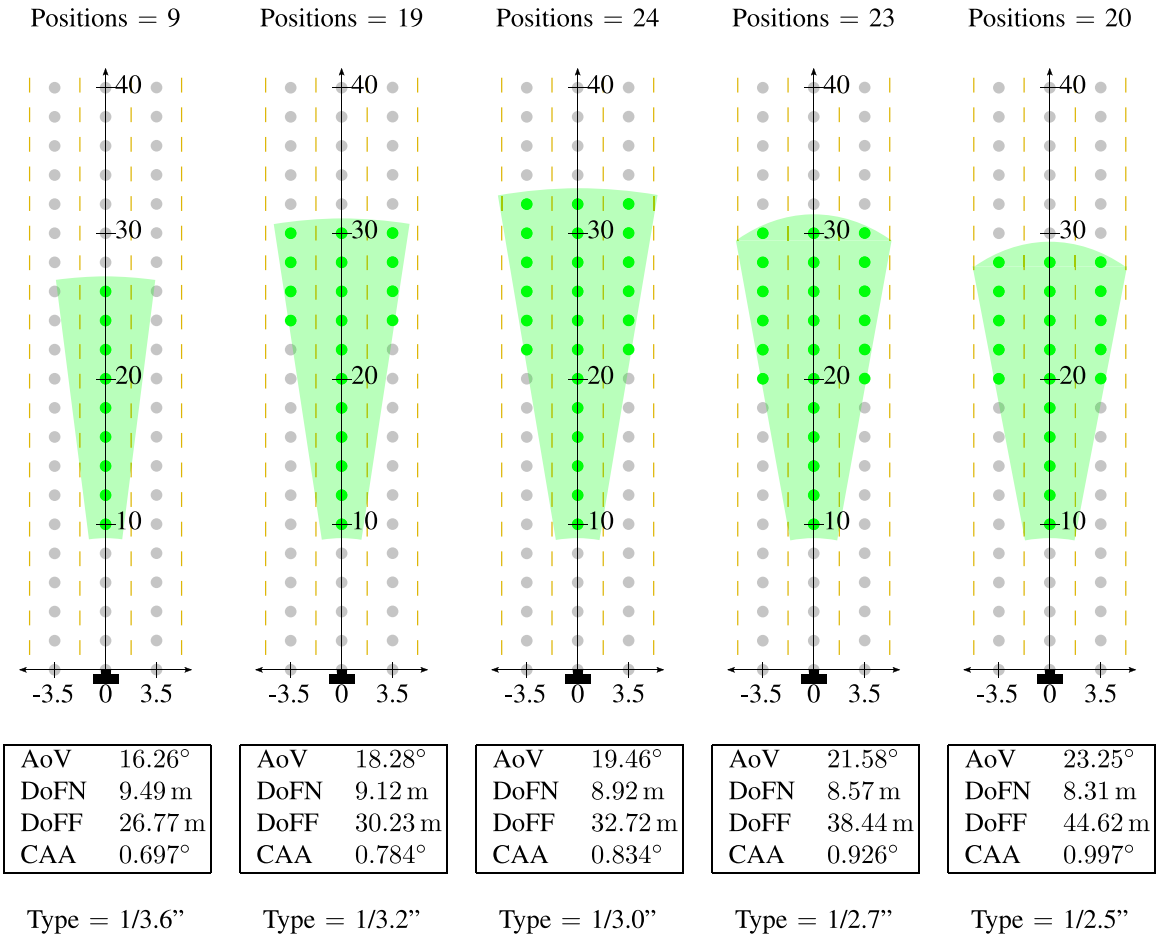

FIGURE 10. Simulated GREs and derived properties for various sensor types (axis in meters).

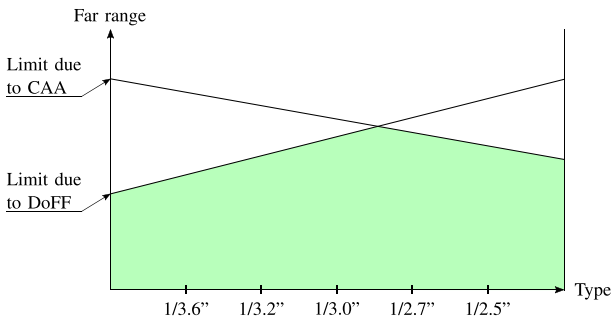

FIGURE 11. The relationship between CAA and DoFF as far range limiting factors for various sensor sizes. The shaded region represents the GRE and is determined by the nearest limiting factor.

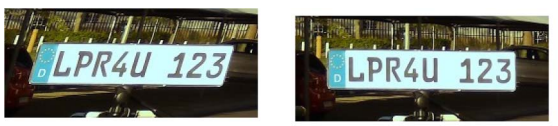

(a) $\dot{\theta} = 12°$, $\phi = 16.79°$ (b) Slant correction applied

FIGURE 12. A license plate captured a high angular velocity exhibiting slant distortion. Successful recognition was achieved after the application of slant correction.

B. ENVIRONMENTAL RESULTS

Results of the lateral motion, yaw rotation and lighting experiments offered great insight into how these factors influence recognition accuracy. Some of the effects observed include slant, motion blur, yaw distortion and lens effects. Each of these effects limited the environmental conditions in which accurate recognition was possible.

1) LATERAL MOTION

The effect of relative lateral motion on recognition accuracy was grouped into the two distortions observed, namely slant and motion blur. Slant distortion occurred due to the use of a progressive scan shutter in the experimental camera and is related to the image sensor readout speed. Motion blur was captured due to the movement of incoming light during photosensor integration.

1) Slant distortion: Twenty different angular velocities ($\dot{\theta}$) were tested and the resultant license plate character slant measured (ϕ). Accurate recognition was achieved up to an angular velocity of 9°/s and approximately 13° of slant. Past this, license plates could be recognized after applying an appropriate amount of slant correction, as shown in Figure 12.

Such high angular velocities typically occur when a vehicle-mounted camera turns through an intersection. This

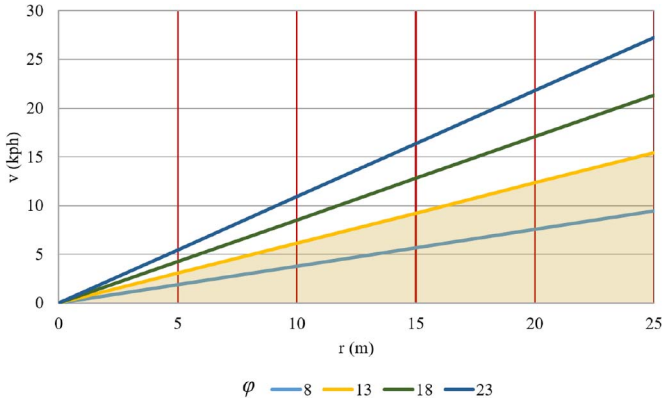

FIGURE 13. Four different degrees of slant observed as a result of camera velocity and turn radius.

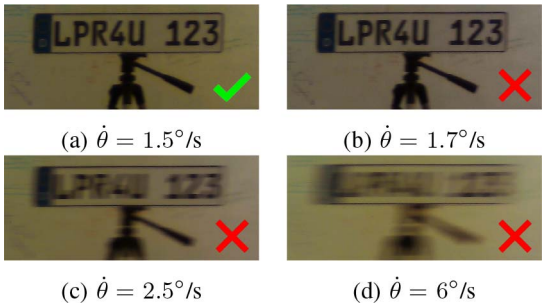

(a) $\dot{\theta} = 1.5°/s$ (b) $\dot{\theta} = 1.7°/s$

(c) $\dot{\theta} = 2.5°/s$ (d) $\dot{\theta} = 6°/s$

FIGURE 14. License plates with lateral motion captured in moderate lighting conditions. The effect of motion blur can be seen and increases with greater angular velocity.

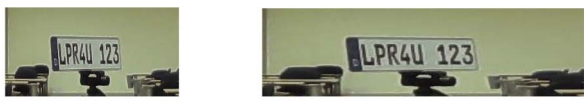

(a) $67.50°$ yaw rotation (b) Stretch correction applied

FIGURE 15. A license plate with $67.50°$ yaw rotation. Successful recognition was achieved after the application of stretch correction.

movement generates slant which can limit recognition accuracy for the full duration of the turn. The amount of slant is proportional to the angular velocity, with the exact factor being dependent on the readout speed of the specific image sensor used. For the experimental camera, this was determined from slant measurements taken at various angular velocities and is shown in Equation (13). The angular velocity of the camera is dependent on its velocity (v) and the turn radius (r), as shown in Equation (14). These two equations were combined into Equation (15) to provide a solution for the approximate amount of slant distortion generated during an arbitrary turn maneuver.

$$\phi \approx 1.325\dot{\theta} \tag{13}$$

$$\dot{\theta} = \frac{180v}{r\pi} \tag{14}$$

$$\phi \approx 238.5\frac{v}{r\pi} \tag{15}$$

This equation was plotted for four different degrees of slant, shown in Figure 13. The shaded region represents velocity and turn radius combinations which produce less than 13° of slant. The experimental camera could theoretically execute such turn maneuvers without impairing recognition accuracy due to slant distortion. The use of slant correction would effectively extend recognition capability to allow accurate recognition in maneuvers with greater velocity and tighter turn radiuses.

2) Motion blur: The prevalence of motion blur differed substantially in bright and moderate lighting conditions due to the automatic adjustment of photosensor integration time. License plates captured in bright lighting conditions revealed no noticeable evidence of motion blur, even at high angular velocities. Conversely, the longer the integration time used in the moderate lighting experiment produced distinct evidence of motion blur.

In such conditions, accurate recognition was achieved only up to an angular velocity of 1.5°/s, as shown in Figure 14. Past this point, character edges became too blurred to be accurately recognized, despite still being legible to the human eye. Characters started to overlap at an angular velocity of 2.5°/s and became indistinguishable at 6°/s.

2) RELATIVE ORIENTATION

The effect of yaw distortion was evident by license plates becoming increasingly horizontally compressed as they were rotated away from the camera. Recognition failed when the license plate was rotated past 45°. This surpassed the 15° limitation of some commercial systems [27].

Although yaw rotation distorted the license plate into a trapezoid shape, the horizontal compression far exceeded the vertical distortion. This allowed for adequate correction of unrecognizable license plates using only image scaling instead of complex planar homography. Scaling the image horizontally restored the license plate's original aspect ratio and enabled successful recognition, as demonstrated in Figure 15.

Theoretically, such correction could be used to remedy the effect of arbitrarily large yaw rotation, provided that the license plate was still captured with sufficient resolution.

3) LIGHTING CONDITIONS

The effect of ambient light intensity already became apparent in the different degrees of motion blur observed during the relative motion experiment. Night-time experiments furthermore highlighted the role of retroflective license plates and vehicle headlights in influencing recognition accuracy.

The non-retroflective license could be recognized up to a range of 10 m, bar a single misidentified character. At this range, the license plate was practically indistinguishable to the human eye, testimony to the remarkable ability of the algorithm to detect edges in night-time conditions. On the other hand, the retroflective license plate was reasonably recognized up to a range of 20 m. This indicates that the use of retroflective license plates approximately double the

night-time recognition range, making it comparable to that achieved in day-time conditions.

Furthermore, on-coming headlights readily produced lens flare and glare which hindered accurate recognition. The extent of these artifacts varied depending on the angle between the on-coming vehicle and camera. Lens flare was present mainly along a specific section of the vehicle's approach, while glare remained as long as the headlights were within the frame.

C. SUMMARY OF RESULTS

Focal length greatly determined far recognition range, as well as coverage of adjacent lanes. The use of a manual focus, or appropriate fixed-focus lens was demonstrated to be sufficient for achieving a large recognition area. Furthermore, a great recognition range was achieved using a high-resolution image sensor of any physical size. Finally, although the aperture size affected recognition area, it would also affect low-light recognition accuracy and should rather be selected based on the lighting conditions in which the camera will typically operate. The model was validated using a representative experiment and found to be an effective tool for estimating the effect of individual camera properties on the recognition area.

In moderate lighting conditions, lateral motion limited recognition accuracy due to motion blur. In bright lighting conditions, a greater amount of lateral motion was tolerable before recognition accuracy was impaired due to slant distortion. Slant correction was demonstrated to effectively enhanced recognition accuracy in bright lighting conditions.

Furthermore, perspective distortion limited the relative orientation between camera and license plate to less than 45° of yaw rotation for accurate recognition to be possible. License plates with a greater amount of yaw rotation could be accurately recognized using a stretch correction technique.

Finally, retroflection was shown to effectively double the range of night-time recognition while oncoming headlights were prone to produced lens effects that were problematic to recognition.

VI. CONCLUSION

This work showed how different optoelectronic and environmental factors significantly affect the recognition accuracy of vehicle-mounted LPR systems.

Optoelectronic factors have a substantial impact on the region in which license plates can be accurately recognized. Although the shape of this region can largely be manipulated using a variable-focus zoom lens, it is possible to achieve a sufficiently large recognition area using an appropriate fixed-focus prime lens. Additional funds should rather be used to invest in a high-resolution image sensor, enabling the recognition of license plates at a much greater distance, although also introducing a greater susceptibility to slant distortion during lateral motion.

Recognition accuracy is impaired in certain environmental conditions too. These include execution of turn maneuvers, license plates orientated at an angle to the camera and oncoming night-time traffic. Nevertheless, the range of night-time recognition approximates that achieved in daylight due to the retroflective characteristic of license plates. Recognition accuracy can also be enhanced to include a greater variation of environmental conditions using image correction techniques, such as slant and stretch correction.

These findings are expected to aid in the selection of an appropriate camera for use in a low-cost multi-agent open-source LPR network in developing countries.

REFERENCES

[1] N. Belen, *Rio's Latest Crime Statistics Show 37 Percent Increase in Auto Theft*, Rio Times, Rio de Janeiro, Brazil, 2017. [Online]. Available: https://riotimesonline.com/brazil-news/rio-politics/rios-latest-crime-statistics-show-mixed-results/

[2] *Crime Stats SA*. Accessed: Dec. 5, 2018. [Online]. Available: http://www.crimestatssa.com/national.php

[3] N. C. R. Bureau, "Crime in India 2016," Government of India, Delhi, India, Rep., 2016. [Online]. Available: https://ncrb.gov.in/crime-india-2016

[4] *How Are Innovations in Technology Transforming Policing?*, Police Executive Res. Forum, Washington, DC, USA, 2012. [Online]. Available: https://web.archive.org/web/20130129220334/http://policeforum.org/library/critical-issues-in-policing-series/Technology_web2.pdf

[5] M. Hoctor. (2012). *Mass Surveillance System Nicks Drivers*. [Online]. Available: https://www.illawarramercury.com.au/story/113726/mass-surveillance-system-nicks-drivers/

[6] D. Bailey, D. Irecki, B. Lim, and L. Yang, "Test bed for number plate recognition applications," in *Proc. 1st IEEE Int. Workshop Electron. Design Test Appl.*, Christchurch, New Zealand, 2002, pp. 501–503. [Online]. Available: http://seat.massey.ac.nz/research/centres/SPRG/pdfs/2002_DELTA_501.pdf

[7] "HTS vehicle recognition solutions VRS M100 imaging unit," Datasheet, HTS, Austin, TX, USA, 2015. [Online]. Available: http://www.htsol.com/wp-content/uploads/2015/06/HTS-Mobile-Enforcement.pdf

[8] "HTS vehicle recognition solutions VRS DR200 imaging units," Datasheet, HTS, Austin, TX, USA, 2014. [Online]. Available: http://www.htsol.com/wp-content/uploads/2014/11/DR-200.pdf

[9] P. Chhoriya, G. Paliwal, and P. Badhan, "Image processing based automatic toll booth in indian conditions," *Int. J. Emerg. Technol. Adv. Eng.*, vol. 3, no. 4, pp. 410–414, 2013. [Online]. Available: https://pdfs.semanticscholar.org/c553/c0b3abf7e4abc69a3d7e711bed58c80fa39d.pdf

[10] L. W. Chen, Y. C. Tseng, and K. Z. Syue, "Surveillance on-the-road: Vehicular tracking and reporting by V2V communications," *Comput. Netw.*, vol. 67, pp. 154–163, Jul. 2014. [Online]. Available: http://dx.doi.org/10.1016/j.comnet.2014.03.031

[11] *Leader in Fixed & Mobile ALPR Systems*, ELSAG, High Point, NC, USA, 2013. [Online]. Available: https://www.elsag.com/

[12] *PIPS Technology—Detection Innovation*, PIPS, San Diego, CA, USA, 2018. [Online]. Available: http://www.pipstechnology.com/

[13] OpenALPR. *Automatic License Plate Recognition*. Accessed: Dec. 5, 2018. [Online]. Available: http://www.openalpr.com/

[14] *JavaANPR—Automatic Number Plate Recognition System*. Accessed: Dec. 5, 2018. [Online]. Available: http://javaanpr.sourceforge.net/

[15] M. Sarfraz, M. Ahmed, and S. Ghazi, "Saudi Arabian license plate recognition system," in *Proc. Int. Conf. Geometric Model. Graph.*, London, U.K., 2003, pp. 36–41. [Online]. Available: http://ieeexplore.ieee.org/document/1219663/

[16] C. T. Nguyen, T. B. Nguyen, and S.-T. Chung, "Reliable detection and skew correction method of license plate for PTZ camera-based license plate recognition system," in *Proc. Int. Conf. Inf. Commun. Technol. Convergence (ICTC)*, Jeju, South Korea, 2015, pp. 1013–1018. [Online]. Available: http://ieeexplore.ieee.org/document/7354726/

[17] L. Liu, S. Zhang, Y. Zhang, and X. Ye, "Slant correction of vehicle license plate image," in *Image Analysis and Processing*. Berlin, Germany: Springer, 2005, pp. 237–244. [Online]. Available: https://doi.org/10.1007/11553595_29

[18] P. S. Ha and M. Shakeri, "License plate automatic recognition based on edge detection," in *Proc. IEEE Artif. Intell. Robot. (IRANOPEN)*, Qazvin, Iran, 2016, pp. 170–174. [Online]. Available: http://ieeexplore.ieee.org/abstract/document/7529509

[19] P. Hurtik and M. Vajgl, "Automatic license plate recognition in difficult conditions—Technical report," in *Proc. Joint 17th World Congr. Int. Fuzzy Syst. Assoc. 9th Int. Conf. Soft Comput. Intell. Syst. (IFSA-SCIS)*, 2017, pp. 1–6. [Online]. Available: http://ieeexplore.ieee.org/document/8023337/

[20] M. C. Rademeyer, M. J. Booysen, and A. Barnard, "Factors that influence the geometric detection pattern of vehicle-based licence plate recognition camera systems," in *Proc. 37th South. Afr. Transp. Conf.*, 2018, pp. 717–727. [Online]. Available: http://hdl.handle.net/2263/69579

[21] D. Malacara and Z. Malacara, *Handbook of Optical Design*, 2nd ed. New York, NY, USA: Marcel Dekker, Inc., 2004. [Online]. Available: http://optdesign.narod.ru/book/Handbook_of_Optical_Design.pdf

[22] D. Hart, *The Camera Assistant: A Complete Professional Handbook*. Boston, MA, USA: Focal Press, 1996. [Online]. Available: https://books.google.co.za/books?id=HjwrBgAAQBAJ

[23] L. Bortner, "Lens equation," Dept. Phys., Univ. Cincinnati, Cincinnati, OH, USA, Rep., 2013. [Online]. Available: https://homepages.uc.edu/∼bortnelj/labs/Physics%203%20experiments/Lens%20Equation/

[24] "HTS vehicle recognition solutions VRS N60L imaging unit," Datasheet, HTS, Austin, TX, USA, 2015. [Online]. Available: http://www.htsol.com/wp-content/uploads/2015/11/N60L.pdf

[25] B. Peterson, *Understanding Exposure: How to Shoot Great Photographs with Any Camera*, 4th ed. Berkeley, CA, USA: Amphoto Books, 2016. [Online]. Available: https://books.google.co.za/books?id=vCDzCQAAQBAJ

[26] B. A. Barsky, *Depth of Field and Hyperfocal Distance Equations and Approximations*. Accessed: Dec. 5, 2018. [Online]. Available: http://inst.eecs.berkeley.edu/∼cs39j/sp05/handouts/depth.of.field.writeup.html

[27] "Troubleshooting LPR issues," GeoVision Inc., Taipei, Taiwan, Rep. GV4-14-06-20-t, 2014. [Online]. Available: http://pd.geovision.tw/faq/AccessControl/LPR_Troubleshoot.pdf

[28] "Camera lens news no. 1," Zeiss, Oberkochen, Germany, Rep. 1, 1997.

[29] J. Kannala and S. Brandt, "A generic camera model and calibration method for conventional, wide-angle, and fish-eye lenses," *IEEE Trans. Pattern Anal. Mach. Intell.*, vol. 28, no. 8, pp. 1335–1340. Aug. 2006. [Online]. Available: https://ieeexplore.ieee.org/document/1642666